ORIGINAL PAPER

Direct electrochemistry and electrocatalysis of nitrite based on nano-alumina-modified electrode

Qiong He · Tian Gan · Dongyun Zheng · ShengShui Hu

Abstract Simple and sensitive electrochemical method for the determination of nitrite, based on a nano-alumina-modified glassy carbon electrode (GCE), is described. Nitrite yields a well-defined oxidation peak whose potential is 0.74 V at the nano-alumina-coated GCE in 0.1 mol L^{-1} phosphate buffer (pH 5.0). Compared with bare GCE, the nano-alumina-modified GCE has evident catalytic effect towards the oxidation of nitrite, and its peak current can be significantly enhanced. Some of the experimental parameters were optimized for the determination of nitrite. The oxidation peak current was proportional to nitrite concentration in the range of 5.0×10^{-8}–1.1×10^{-3} mol L^{-1}, and a detection limit of 1.0×10^{-8} mol L^{-1} was obtained. This method has been successfully used to the determination of nitrite in sausage sample. Furthermore, results obtained by the method have been compared with spectrophotometric method.

Keywords Nano-alumina · Modified electrode · Nitrite · Electrocatalysis

T. Gan · D. Zheng · S. Hu (✉)
College of Chemistry and Molecular Sciences, Wuhan University,
Wuhan 430072, China
e-mail: sshu@whu.edu.cn

Q. He
Department of Chemistry, Qujing Normal College,
Qujing 655011, China

Q. He · S. Hu
State Key Laboratory of Transducer Technology,
Chinese Academy of Sciences,
Beijing 100080, China

Introduction

As is well known, nitrite is common in environment, physiological systems, and usually as the additive of food [1]. Its reaction with dietary components in the stomach forms toxic and carcinogenic nitrosamines [2–4]. So as its potential toxicity, its determination is then important for environmental reason and for public health. Some methods such as spectroscopic analysis [5–7] and chromatography [8,9] methods have been used in the determination of nitrite. Davis and coworkers have made a review focused on the use of these techniques on environmental nitrite analysis [10]. However, developing electrochemical methods with high quality to determine nitrite has been paid much attention because of their quick response, high sensitivity, and readily miniaturized [11–16]. While those methods that used chemically modified electrodes also have some limitation [17], such as lower sensitivity and unstable modified film, some have not been applied in real samples [18,19].

Nanomaterials have attracted extensive attention in the recent years due to their unique structures and catalytic properties. The modification of an electrode by nano-structured materials is an essential way to enhance the determination sensitivity of the electrochemical method. Some metal oxide nanomaterials, e.g., nano-alumina, a nanometer material, has been widely used in electrochemical sensors and electroanalysis. In early work, Zak and Kuwana reported [20] that the presence of alumina particles dispersed on a glassy carbon surface would strongly adsorb compounds and catalyze their oxidation. Recently, a nano-alumina-modified glassy carbon electrode (GCE) has been used in the detection of NO and has obtained satisfactory results [21]. To our best knowledge, up until now, there is no report using the nano-Al$_2$O$_3$ modified glassy carbon electrode to detect nitrite in the solution.

In this work, a simple procedure is described for coating nano-alumina on glassy carbon electrode, and a novel electrochemical method for the determination of nitrite is developed. Advantages of the new method are the convenience to prepare nano-Al_2O_3-modified GCE and its high current response for the oxidation of nitrite due to large surface area and catalytic effect of nano-Al_2O_3. Satisfactory linear range and detection limit were obtained, and this method could be well applied to the determination of nitrite in real sample.

Experimental

Reagents and chemicals

All chemicals were of analytical-reagent grade unless otherwise stated and used without further purification. The water used in this work is redistilled.

Nano-alumina was purchased from Shanghai Reagent Factory (Shanghai, China), and other reagents were used as received. A 1.0×10^{-2}-mol L^{-1} stock solution of nitrite was prepared by direct dissolution of sodium nitrite in water and stored in the dark.

Apparatus

All the electrochemical measurements were carried out using a CHI 830 electrochemical analyzer (Shanghai Chenhua Co., China). A conventional three-electrode system, consisting of a nano-alumina-modified GCE (3 mm in diameter), a saturated calomel reference electrode, and a platinum wire auxiliary electrode, was employed. Use TU1810 UV-Vis spectrophotometer (Beijing Purkinje General Instrument Co., Ltd., China) for comparison in real sample analysis.

Fabrication of nano-alumina-modified GCE

The glassy carbon electrode was first rinsed for 3 min with 1:1 HNO_3, ethanol, and redistilled water, respectively. Then, we hand ground on the microcloth pads with alumina (0.05 μm) slurry for 80 s, rinsed with redistilled water, and finally allowed to dry in air. The obtained modified electrode was denoted as nano-Al_2O_3-modified GCE that was used as NO_2^- sensor.

Analytical procedure

Unless otherwise stated, 0.1 mol L^{-1} phosphate buffer (pH 5.0) was used as determining medium for nitrite analysis. The differential pulse voltammograms were recorded from 0.40 to 1.20 V with the following parameters: amplitude=0.1 V, pulse width=0.05 s. Finally, the oxidation peak currents were individually measured.

Sample preparation

The preparation of real sample was carried out according to the national detection standards of People's Republic of China—the determination method of nitrite and nitrate in food (the first law) (GB/T 5009.33-1996). The sausage sample used in the experiment was bought from the local market. About 10.0 g of the sample was weighed, cut with a clean scissors, and grinded to uniform in a mortar. Then, the sample was put to a 100-mL beaker and mixed with 70 mL water and 12 mL NaOH (0.5 mol L^{-1}).The pH of the solution was adjusted to 8.0 with NaOH and H_2SO_4 (both are 0.5 mol L^{-1}) and then transferred to a 250-mL flask quantitatively following with 10.0 mL zinc sulfate (0.42 mol L^{-1}) added to deposit protein. The flask was put in 60 °C water bath for 10 min, and adequate water was added to the mark when the flask was cooled to room temperature. It was kept still for 30 min. Whereafter, the fat floating above the solution was removed, and the residual solution was filtered. The first 50-mL filtrate was abandoned, and the subsequent filtrate was collected together and kept in refrigerator.

Results and discussion

Surface morphology of different electrodes

The surface morphologies of GCE and nano-Al_2O_3-film-modified GCE are characterized by SEM (Fig. 1). As shown in Fig. 1a, the surface of GCE is very smooth. Many nanoparticles can be observed on the surface of nano-Al_2O_3-modified GCE, as shown in Fig. 1b. The nano-Al_2O_3 forms compact and uniform film with plenty of micropores of nanosizes that allow the free entry of substrates to the inner of nano-Al_2O_3 film.
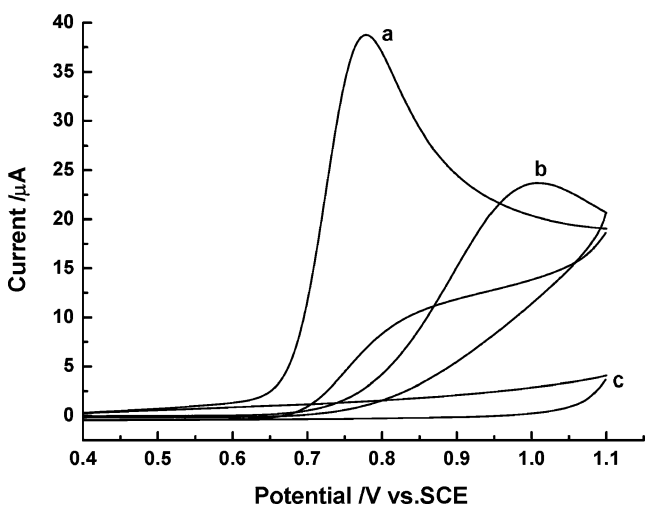
Electrocatalytic oxidation of nitrite

The electrochemical behaviors of nitrite at the bare GCE and nano-Al_2O_3-modified GCE were investigated using cyclic voltammetry. Figure 2 shows the cyclic voltammograms of 1.0×10^{-3} mol L^{-1} NO_2^- in 0.1 mol L^{-1} phosphate buffer (pH 5.0). During the anodic potential sweep from 0.40 to 1.10 V, two oxidation peaks are observed at about 1.00 V on the bare GCE (b) and 0.78 V on the nano-Al_2O_3-modified GCE (a), respectively. On the following reverse sweep, no corresponding reduction peak is observed on both electrodes, suggesting that the electrode processes of nitrite on the bare GCE and nano-Al_2O_3-modified GCE are totally irreversible.
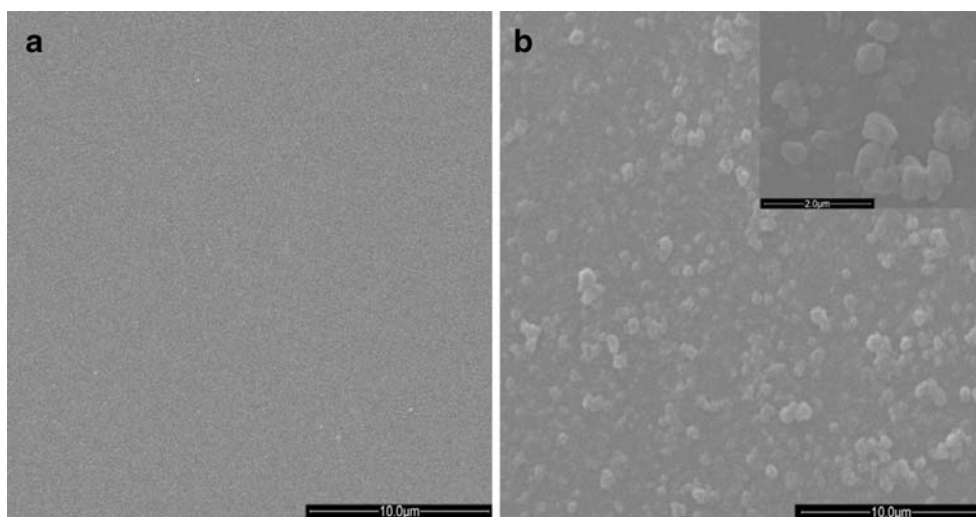
The cyclic voltammetric response of the nano-Al$_2$O$_3$-modified GCE in 0.1 mol L^{-1} phosphate buffer (pH 5.0) without nitrite is depicted as Fig. 2c. The curve is very smooth during the cyclic potential sweep from 0.40 to 1.10 V.
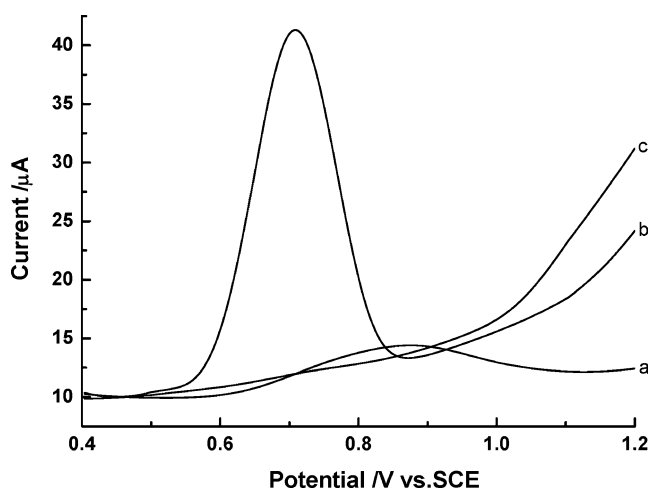
From the comparison of curves (a) and (b), it is very clear that the oxidation potential shifts more negatively at the nano-Al$_2$O$_3$ electrode, which demonstrated that the modified electrode can catalyze the oxidation of nitrite. And the peak current of nitrite increased significantly at the modified electrode, further implying that nano-Al$_2$O$_3$-modified GCE held the properties that were favorable to the oxidation of nitrite. The nano-Al$_2$O$_3$-modified GCE has larger surface area (e.g., a larger electrochemical reaction interface) compared with the bare GCE, which undoubtedly can adsorb more NO$_2^-$ onto the surface of the electrode and, therefore, shows better performance towards nitrite.

We have also studied the electrocatalytic oxidation of nitrite by differential pulse voltammetry (DPV) for it is an ideal technique for electrochemical detection with high sensitivity and excellent resolution. At the condition of without accumulation, an oxidation peak is observed for 8.0×10^{-4} mol L^{-1} nitrite at 0.87 V at the bare GCE (Fig. 3a). The oxidation peak current is very low, suggesting that the bare GCE possesses poor activity to the electrochemical oxidation of nitrite.

Figure 3b shows the DPV response of 8.0×10^{-4} mol L^{-1} nitrite at the nano-Al$_2$O$_3$-modified GCE without accumulation. A sensitive and well-defined oxidation peak appears at 0.74 V during the potential sweep from 0.40 to 1.20 V. And Fig. 3c depicts the DPV behavior of the nano-Al$_2$O$_3$-film-modified GCE in 0.1 mol L^{-1} phosphate buffer (pH 5.0). From the comparison of curves (a) and (b), both considerable peak current enhancement and more negative peak potential are observed, which suggest that nano-Al$_2$O$_3$

Fig. 2 Cyclic voltammograms of 1×10^{-3} mol L^{-1} NO$_2^-$ in pH 5.0 phosphate buffer at nano-Al$_2$O$_3$-film-modified GCE (**a**) and bare GCE (**b**). **c** Nano-Al$_2$O$_3$-film-modified GCE in buffer without NO$_2^-$. Scan rate=100 mV s^{-1}

Fig. 3 Dfferential pulse voltammetry responses of 8×10^{-4} mol L^{-1} NO$_2^-$ at **a** bare GCE; **b** nano-Al$_2$O$_3$-film-modified GCE; **c** nano-Al$_2$O$_3$-film-modified GCE in buffer without NO$_2^-$

Fig. 4 Cyclic voltammograms of nano-Al$_2$O$_3$-film-modified GCE in the 0.1 mol L^{-1} phosphate buffer (pH5.0) containing 1×10^{-3} mol L^{-1} NO$_2^-$ at different scan rates (from inner to outer—25, 50, 75, 100, 150, 200, 250, 300, 350, 400, 450 and 500 mV s^{-1}, respectively). *Insert A* plot of the dependence of the peak current on the square root of scan rates. *Insert B* plot of the dependence of the peak potential on the scan rates
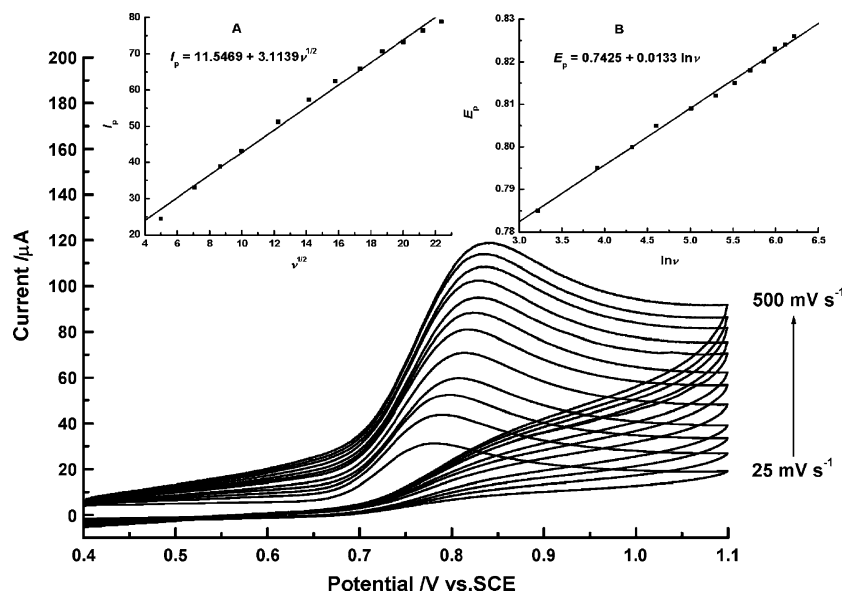
exhibits an excellent catalytic effect towards the oxidation of nitrite again. Thus, conclusion can be made from the comparison that nano-Al$_2$O$_3$-modified GCE is more active to nitrite and can greatly improve the determination sensitivity of nitrite.

Effect of scan rate

The relationship between the oxidation peak current of 1.0×10^{-3} mol L^{-1} nitrite and scan rate was studied using cyclic volammetry (Fig. 4). It is found that the oxidation peak current at nano-Al$_2$O$_3$-modified GCE increases linearly with the square root of the scan rate over the range from 25 to 500 mV s^{-1} (Fig. 4, insert A), which suggested that the oxidation of nitrite was diffusion-controlled. Moreover, the oxidation peak potential linearly shifts positively when increasing the scan rate (Fig. 4, insert B), $E_p = 0.7425 + 0.0133 \ln v$, $R=0.998$, also indicating that the electrode process of nitrite is totally irreversible. For an irreversible process, the relationship between the peak potential (E_p) and scan rate could be represented by equation [22]:

$$E_p = K + \frac{RT}{2(1-\alpha)n_\alpha F} \ln v \qquad (1)$$

$$K = E^{0'} + \frac{RT}{(1-\alpha)n_\alpha F}$$
$$\times \left[0.78 + \frac{1}{2}\ln\left(\frac{(1-\alpha)n_\alpha FD}{k^2 RT} \right) \right] \qquad (2)$$

where α is transfer coefficient, n_α is the number of electrons involved in the rate-determining step, v is scan

rate, $E^{0'}$ is standard electrode potential, k is heterogeneous electron transfer constant, and D is diffusion coefficient. From the results, we could calculate that $(1-\alpha)n_\alpha$ is 0.965, and generally, α in the totally irreversible electrode process is assumed as 0.5. Consequently, two electrons are involved in the oxidation of NO$_2^-$.

Influence of some experiment conditions

Influence of electrolyte pH

By changing the pH of the phosphate buffer from 4.0 to 7.0, the DPV behaviors of NO$_2^-$ at nano-Al$_2$O$_3$-modified GCE were studied, shown in Fig. 5. Because the pK_a of HNO$_2$ is 3.3, NO$_2^-$ exists as ions in the pH range of 4.0–
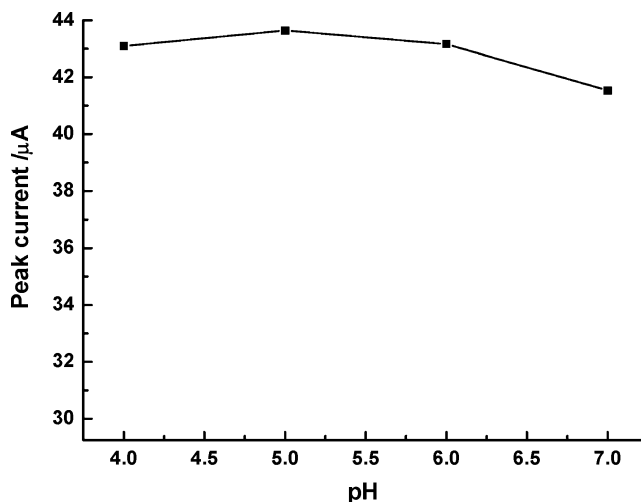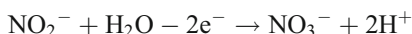

Fig. 5 Influence of pH value on oxidation peak current of 1×10^{-3} mol L^{-1} NO$_2^-$ in 0.1 mol L^{-1} phosphate buffer
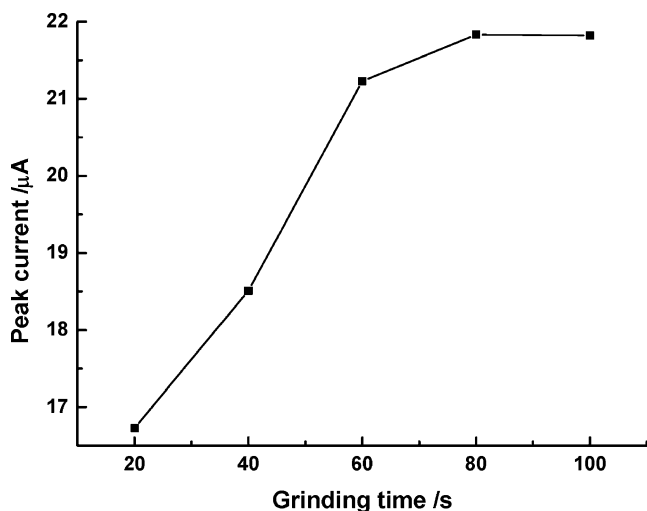
Fig. 6 Influence of the grinding time on oxidation peak current of 5×10^{-4} mol L^{-1} NO_2^- in 0.1 mol L^{-1} phosphate buffer (pH5.0)

7.0, the reaction on the electrode surface can be expressed as follows [23]:

$$NO_2^- + H_2O - 2e^- \rightarrow NO_3^- + 2H^+$$

In pH4.0 phosphate buffer, the peak potential of 1.0×10^{-3} mol L^{-1} NO_2^- is about 0.732 V, and the peak current is 43.102 μA; when pH increases to 5.0, the peak potential of NO_2^- shifts positively about 8 mV, and the peak current is 43.668 μA; whenever pH is 6.0 or 7.0, the peak potential is 0.734 V, and the peak current is 43.191 and 41.547 μA, respectively. From which, it can be seen that pH has little influence on the peak potential of NO_2^- and its oxidation peak current. But for the reason of determination sensitivity, 0.1 mol L^{-1} phosphate buffer (pH5.0) was chosen as the supporting electrolyte.

Influence of the grinding time

The influence of grinding time is also studied because it is supposed that this can affect the combination of nano-alumina film and the GCE surface and then the electrochemical responses to nitrite. If the GCE is ground for a too short time, such little nano-Al_2O_3 can be adhered to the surface of GCE, and the combination between nano-Al_2O_3 and electrode will be so weak, which disables the nano-Al_2O_3 from using its super properties fully. But when GCE is ground for a too long time, too much nano-Al_2O_3 will conglutinate on the electrode, which can inhibit the electron transfer between NO_2^- and the electrode and then affect the determination sensitivity of NO_2^-. The influence of grinding time on the peak current of 5.0×10^{-4} mol L^{-1} NO_2^- is demonstrated in Fig. 6, which shows that when the GCE is ground for 80 s, then the highest peak current is obtained for the determination of nitrite.

Influence of the initial potential

In electrochemical determination, initial potential is an important parameter which can influence the peak current of NO_2^-. In this work, the effects of initial potential on the oxidation peak current of NO_2^- were investigated. In order to evaluate the influence of initial potential on the determination of NO_2^-, the oxidation peak currents of 5.0×10^{-4} mol L^{-1} NO_2^- under different initial potentials were measured by DPV (Fig. 7). It is found that the oxidation peak current increases dramatically when the initial potential changes from −0.2 to 0.0 V for the reason that the more positive potential can provide the increased driving force for the fast oxidation of nitrite but changes slightly as changing from 0.0 to 0.5 V. Thus, the initial potential was performed at 0.4 V for the sake of convenience.

Chronoamperometric measurements

Chronoamperometry was also used to investigate the electrode process of NO_2^- at the nano-Al_2O_3-film-modified GCE (Fig. 8a) and bare GCE (Fig. 8b). The plots of charge against the square root of time (Q–$t^{1/2}$) show a linear relationships at nano-Al_2O_3-modified GCE (curve a′) and bare GCE (curve b′) in the presence of 5.0×10^{-4} mol L^{-1} NO_2^- (Fig. 8, insert A). According to the integrated Cottrell equation [24], the relationship between Q and $t^{1/2}$ can be described as follows:

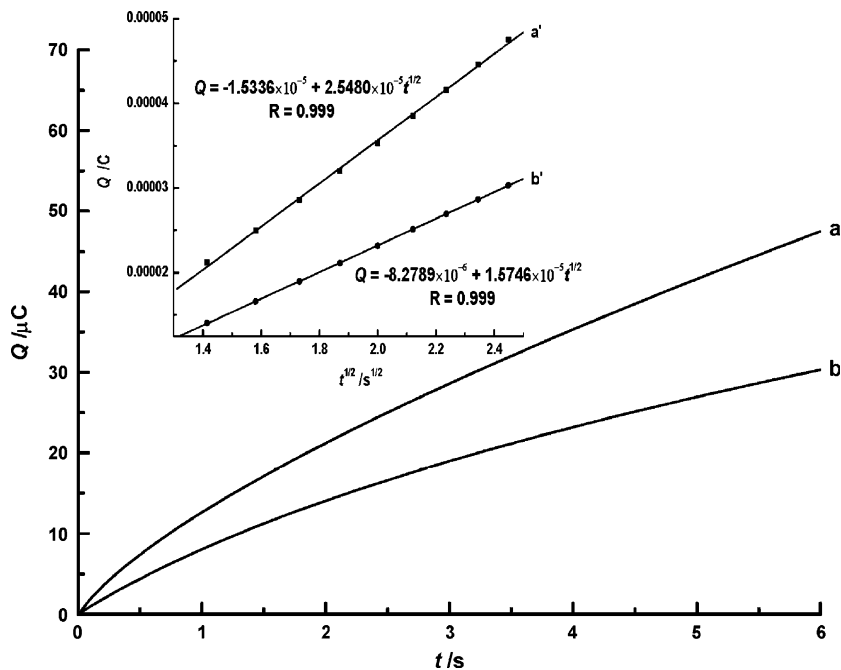$$Q = 2n_\alpha cFAD^{\frac{1}{2}}t^{\frac{1}{2}}\pi^{-\frac{1}{2}} + Q_{dl} + Q_{ads} \tag{3}$$

$$Q_{ads} = n_\alpha FA\Gamma \tag{4}$$

where A is the electrode area, c is the concentration of NO_2^-, D is the diffusion coefficient, Q_{dl} is the double layer
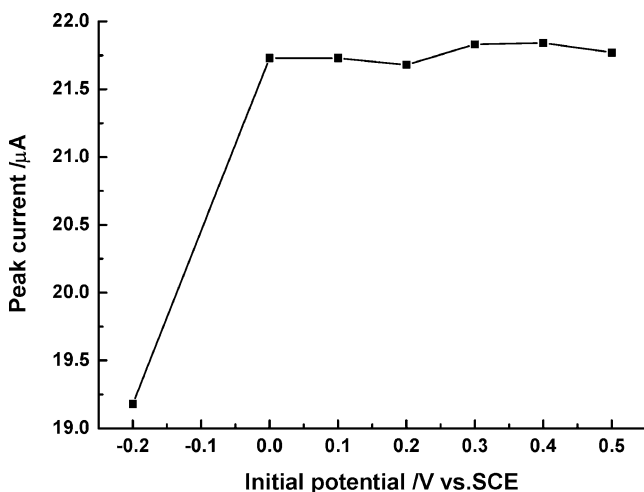
Fig. 7 Influence of the initial potential on oxidation peak current of 5×10^{-4} mol L^{-1} NO_2^- in 0.1 mol L^{-1} phosphate buffer (pH5.0)

charge, Q_{ads} is the adsorption charge, Γ is the surface coverage, and other symbols have their usual significances. Considering $n_\alpha = 2$, A=0.071 cm^2, c=5×10^{-4} mol L^{-1}, π= 3.14, F=96,500 C mol^{-1}, according to Eq. 3, we can calculate that D is 4.15×10^{-6} and 1.09×10^{-5} cm^{2}s^{-1} for bare GCE and nano-Al_2O_3-modified GCE, respectively. According to Eq. 4, we can calculate that Γ is 6.04×10^{-10} and 1.12×10^{-9} mol cm^{-2} for bare GCE and nano-Al_2O_3-modified GCE, respectively. From these results, it is clear

that nano-Al_2O_3 film leads to faster and more amount of adsorbed (i.e., the surface coverage) of NO_2^- at nano-Al_2O_3-modified GCE than that at bare GCE.

Amperometric detection of NO_2^-

In order to examine the responses character of nano-Al_2O_3-modified GCE to NO_2^-, we performed the detection of NO_2^- in a stirred 0.1 mol L^{-1} phosphate buffer (pH5.0) with constant

Fig. 9 Amperometric response of NO_2^- at nano-Al_2O_3-film-modified GCE with successive injections of different NO_2^- concentrations at the operational potential of 0.80 V. Insert A plot of the dependence of the oxidation peak current on NO_2^- concentrations. Insert B amplificatory image of the figure from 50 to 790 s
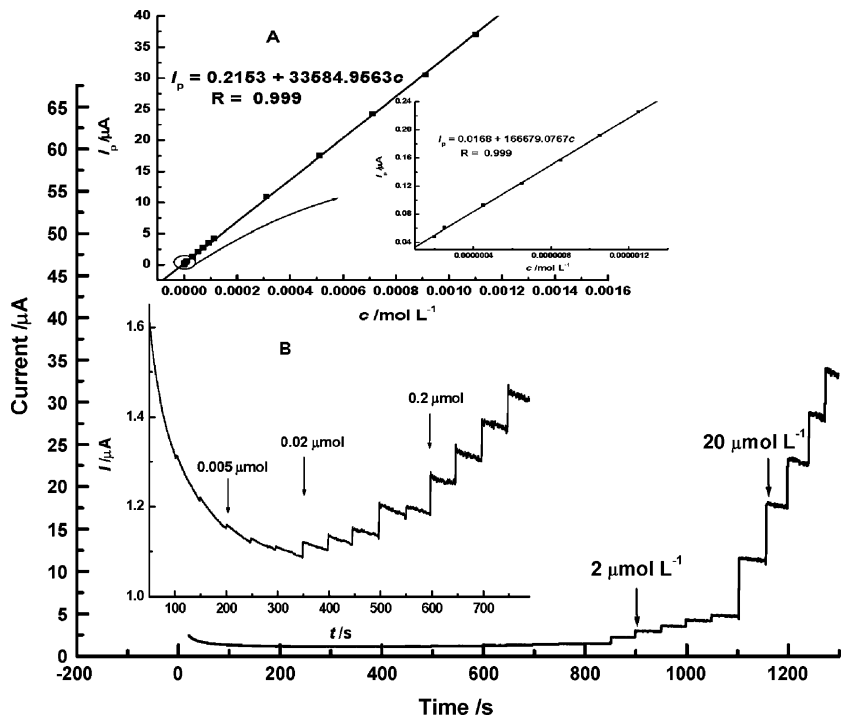
Table 1 The influences of some ions on the peak current of 5.0×10^{-4} mol L^{-1} NO_2^- in 0.1 mol L^{-1} phosphate buffer (5.0) at nano-Al_2O_3-film-modified GCE

Interferents	Concentration (mol L^{-1})	Signal change (%) (μA)
Na^+	1.0×10^{-1}	0
K^+	1.0×10^{-1}	0
Mg^{2+}	1.0×10^{-1}	−0.56
Al^{3+}	1.0×10^{-1}	0.48
Zn^{2+}	1.0×10^{-1}	0
Ba^{2+}	1.0×10^{-1}	0
Cl^-	1.0×10^{-1}	0
SO_4^{2-}	1.0×10^{-1}	1.68
Hg^{2+}	5.0×10^{-2}	−1.23
Cd^{2+}	5.0×10^{-2}	1.34
Cu^{2+}	5.0×10^{-2}	−1.08
Pb^{2+}	5.0×10^{-3}	4.32
SO_3^{2-}	5.0×10^{-4}	43.23
I^-	5.0×10^{-4}	23.6
CO_3^{2-}	5.0×10^{-4}	19.86
HCO_3^-	5.0×10^{-4}	16.58

potential. Fig. 9 shows a typical amperometric response for the determination of NO_2^- at a potential of +0.80 V for each successive addition of different concentrations of NO_2^- to 0.1 mol L^{-1} phosphate buffer (pH5.0). We can see that nano-Al_2O_3-modified GCE exhibits rapid responses to the changes in NO_2^- concentration. According to this experiment, a linear relationship between peak currents and NO_2^- concentrations was obtained in the range of 5.0×10^{-8} to 1.1×10^{-3} mol L^{-1} with a correlation coefficient $R=0.999$. The detection limit was estimated to be 1.0×10^{-8} mol L^{-1}.

The stability and reproducibility of nitrite sensor

It was observed that the nano-Al_2O_3-modified GCE remains 96% of its initial response to NO_2^- after it was kept in air for 2 weeks, which indicates that the modified electrode has good stability. To prove the reproducibility of the method, electrochemical experiments were repeatedly performed 10 times with the different nano-Al_2O_3-modified GCEs in the solution containing 5.0×10^{-4} mol L^{-1} NO_2^-. The relative standard deviation was calculated to be 2.23%,

which revealed that the repeatability of the nano-Al_2O_3-modified GCE was excellent.

Interference

We also examined possible interferences from other ions and molecules on the NO_2^- detection at the nano-Al_2O_3-modified GCE by addition of various ions into the 0.1 mol L^{-1} phosphate buffer (pH5.0) containing 5.0×10^{-4} mol L^{-1} nitrite. If addition of a given molecule causes a current change of 10% or more, we consider it to be interfering. We found that Na^+, K^+, Mg^{2+}, Al^{3+}, Zn^{2+}, Ba^{2+}, Cl^-, SO_4^{2-}, do not interfere with NO_2^- detection in a 200-fold concentration. A hundred-fold Hg^{2+}, Cd^{2+}, and Cu^{2+} and 10-fold Pb^{2+} do not interfere with NO_2^- detection, but 1-fold amount of I^-, SO_3^{2-}, CO_3^{2-}, and HCO_3^- exhibit serious interference, as shown in Table 1. The results indicate that this modified electrode may have potential for the monitoring of NO_2^- in real samples.

Sample analysis

This method is applied to the determination of nitrite in sausage sample. A 0.1-mL prepared sausage sample solution was placed in 10 mL 0.1 mol L^{-1} phosphate buffer (pH5.0) and then determined the nitrite in the solution using DPV model. In order to estimate the accuracy of this method, results obtained by nano-Al_2O_3-modified GCE were compared with those determined by spectrophotometry. The comparison is shown in Table 2. It is found that the results obtained by these two methods are very similar to each other, suggesting that nano-Al_2O_3-modified GCE has great potential to practical sample analyses. Further, in order to establish the suitability of the proposed method, known amounts of the standard NO_2^- were added to the analytical solution of the sausage sample, and the procedure was applied. Recoveries are 98.7% and 100.4%, indicating that the accuracy and repeatability of the proposed voltammetric method are good.

Conclusions

In this work, a nano-Al_2O_3 film modified GCE was prepared through a simple grinding treatment. Nano-

Table 2 Determination of NO_2^- in sausage sample

Sample	Added (mg kg^{-1})	Expected (mg kg^{-1})	Found (mg kg^{-1})	RSD (%)	Recovery (%)	UV (mg kg^{-1})	RSD (%)
Sausage	0.0	–	6.09	5.57	–	6.06	3.47
	3.0	9.09	8.97	4.26	98.7		
	5.0	11.09	11.14	3.98	100.4		

RSD relative standard deviation

Al_2O_3 provides a larger surface area and the adsorptive property for the electrode as well as more catalytic ability for NO_2^- oxidation, due to its small dimensions and porous structure, the nano-Al_2O_3-film-modified GCE remarkably enhances the oxidation peak current of nitrite as well as its determining sensitivity.

References

1. Sun JQ, Sun YP, Wang Z, Sun CQ, Wang Y, Zhang X, Shen JC (2001) Macromol Chem Phys 202:111–116
2. Mirvish SS (1995) Cancer Lett 93:17–48
3. Wolf IA, Wasserman AE (1972) Science 177:15–19
4. Walters CI (1980) Oncology 37:289–296
5. Moorcroft MJ, Davis J, Compton RJ (2001) Talanta 54:785–803
6. Frenzel W, Schulz-Brussel J, Zinvirt B (2004) Talanta 64:278–282
7. Arias-Negrete S, Jimenez-Romero LA, Soliis-Martiinez MO, Ramiirez-Emiliano J, Avila EE, Cuella-Mata P (2004) Anal Biochem 328:14–21
8. Siu DC, Henshall A (1998) J Chromatogr A 804:157–160
9. Helaleh MIH, Korenaga T (2000) J Chromatogr B 744:433–437
10. Dutt J, Davis J, Environ J (2002) Monit 4:465–471
11. Geng RG, Zhao GH, Liu MC, Li MF (2008) Biomaterials 29:2794–2801
12. Jiang LY, Wang RX, Li XM, Jiang LP, Lu GH (2005) Electrochem Commun 7:597–601
13. Doménech A, Torres FJ, Alarcón J (2004) Electrochim Acta 49:4623–4632
14. Xie F, Li WJ, He JL, Yu SF, Fu T, Yang H (2004) Mater. Chem Phys 86:425–429
15. Tau P, Nyokong T (2007) J Electroanal Chem 611:10–18
16. Liu PF, Hu JH (2002) Sens Actuators B, Chem 84:194–199
17. Li J, Xu JR, Sun XY (2002) Chin J Anal Chem 30:206–209
18. Caro CA, Bedioui F, Zagal JH (2002) Electrochim Acta 47:1489–1494
19. Zhao YD, Zhang WD, Luo QM (2003) Microchem J 75:189–192
20. Zak J, Kuwana T (1982) J Am Chem Soc 104:5514–5515
21. He Q, Zheng DY, Hu SS (2009) Microchim Acta 164:459
22. Bard AJ, Faulkner LR (1980) Electrochemical methods: fundamentals and application. Wiley, New York
23. Pei JH, Li XY (2000) Talanta 51:1107–1115
24. Bard AJ, Faulkner LR (2001) Electrochemical methods: fundamentals and application. Wiley, New York